Structure Development of Poly(L-lactic acid) Fibers Processed at Various Spinning Conditions

Subhas Ghosh,[1] Nadarajah Vasanthan[2]

[1]*School of Technology Studies, Eastern Michigan University, Ypsilanti, Michigan 48197*
[2]*Department of Chemistry, Long Island University, Brooklyn, New York 11201*

Received 11 July 2005; accepted 29 November 2005
DOI 10.1002/app.24104
Published online in Wiley InterScience (www.interscience.wiley.com).

ABSTRACT: Poly(L-lactic acid) (PLA) filaments were spun by melt-spinning at 500 and 1850 mm^{-1}, and further drawn and heat-set to modify the morphology of these PLA filaments. PLA yarns were characterized by wide-angle X-ray diffraction (WAXD) and sonic method. WAXD reveals that PLA yarns spun at 500 mm^{-1} are almost amorphous while the PLA filaments spun at 1850 mm^{-1} have about 6% crystallinity. This is different from PET filaments spun at the same speed that have almost no crystallinity. Both drawn- and heat-set PLA filaments showed much higher crystallinity (60%) than do as-spun fibers produced at 500 and 1850 mm^{-1} speed, which is also higher than the usual heat-set PET yarns. It appears that crystalline orientation rapidly reaches a value in the order of 0.95 at 1850 mm^{-1} and that drawn- and heat-set yarns have almost the same crystalline orientation values. Molecular orientation is relatively low for as-spun PLA yarn, and molecular orientation increased to ~0.5 after drawing or heat–setting or both. © 2006 Wiley Periodicals, Inc. J Appl Polym Sci 101: 1210–1216, 2006

Key words: Poly(lactic acid); thermoplastic; optical isomer; morphology

INTRODUCTION

Poly(L-lactic acid) (PLA) fibers by Cargill show a great potential for the production of textile fabrics, furnishing fabrics, automotive interior materials, and medical devices.[1–3] PLA polymers are derived from starch present in corn that are produced by fermentation in the current process. Lactic acid is commercially produced from corn, which is then polymerized to produce PLA. The development of PLA can be traced back to the year 1932, when Carothers produced a low-molecular weight product. His approach to produce PLA from lactic acid monomer includes the removal of water from condensation, using solvent, under high vacuum and heat. This was followed by the development of medical applications of PLA by DuPont and Ethicon for products, such as sutures, implants, and controlled drug release products. Recently, Cargill developed a fermentation process of dextrose from corn that has reduced the cost of manufacturing the lactic acid monomer. Cargill's approach is to remove water under a milder condition, without solvent, which produces a cyclic dimer, lactide. The monomer is purified by vacuum distillation, followed by ring-opening polymerization under heat.[4]

An important feature of PLA, the one that provides a great opportunity for the precise control of fiber structure and properties, is that it can be obtained in two optically active forms. The L-lactic acid isomer rotates the plane of light in a clockwise direction, and the D-isomer rotates it in a counterclockwise[4] direction. The ratio of these two forms and also an optically inactive meso form in the production of the cyclic lactide intermediate is controllable, and the ring-opening polymerization permits the production of PLA resin of different isomer ratios and molecular weights. PLA with more than 15% D-isomer content does not crystallize, whereas the L form is crystallizable. Isomeric forms of lactide are illustrated in Figure 1. Preparation of PLA fibers has been studied more recently, because of its application on micro surgery and composites.[5–7] The final properties of these fibers depend on processing conditions.

This thermoplastic polymer produced from renewable crops is combustible like natural fibers, and its thermoplasticity provides a great advantage in a number of products, including automotive interior material and parts, as it conforms to various shapes. PLA is stable in natural conditions of temperature and humidity; however, degradation begins at 60°C and 90% relative humidity. It is possible to degrade PLA into water and carbon dioxide by hydrolysis.[8] This degradability is important for disposal, particularly, in densely populated areas and in landfills. For several applications, the relatively low glass transition temperature (T_g) and low modulus of PLA are disadvantageous. PLA also suffers from an unfavorable rate of hydrolysis above T_g.[9] This article describes the study

Correspondence to: S. Ghosh (subhas.ghosh@emich.edu).

Journal of Applied Polymer Science, Vol. 101, 1210–1216 (2006)

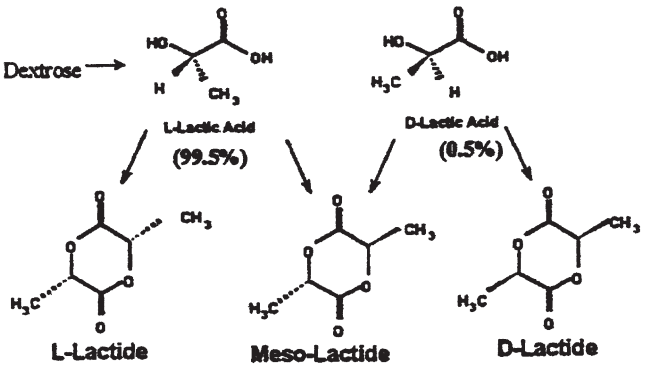

Figure 1 Lactide intermediates from lactic acid.

of PLA filament's structural and morphological changes arising from the changes in filament spinning conditions and potential modification of T_g by adding clay nano particles.

EXPERIMENTAL

Yarn samples

PLA fibers were obtained by the melt-spinning method. Processing conditions used for those PLA filaments that are utilized for structural and morphological studies are listed later. Heat-setting was carried out at constant length.

i. Spinning speed of 500 mm^{-1} (as-spun sample).
ii. Spinning speed of 500 mm^{-1} (drawn, heat-set, and relaxed).
iii. Spinning speed of 1850 mm^{-1} (as-spun filaments).
iv. Spinning speed of 1850 mm^{-1} (drawn, heat-set with tension on roll (no relaxation)).
v. Spinning speed of 1850 mm^{-1} (drawn, heat-set, and relaxed). All yarns were 200 d after drawing.

Thermal analysis

Isothermal crystallization and melting behavior of various fiber samples were measured with Perkin–Elmer differential scanning calorimeter (DSC 7). The instrument was calibrated using indium and zinc, at several times, during these measurements. Onset values were used as melting and crystallization temperatures. The samples were heated 20°C above the melting temperature and cooled down rapidly to a predetermined crystallization temperature for isothermal crystallization and cooled at the rate of 10°C min^{-1} for nonisothermal crystallization.

Wide angle X-ray diffraction

Wide angle X-ray diffraction (WAXD) of PLA fibers revealed the existence of two crystal modifications. The structure of α crystal modification is pseudo orthorhombic exhibiting 10/3 helical conformation, and the β crystal form exhibits 3/1 helical conformation.[5–7] A counter X-ray diffractometer was used to produce diffracted intensity profiles, to determine crystalline fraction, crystal size (CS), and crystalline orientation of the filaments. Furthermore, sonic moduli of these filaments were measured to estimate molecular orientation. It appeared from the diffraction photograph of PLA samples that the PLA unit cell has an orthorhombic form. The 2θ position is for the hkl lattice, showing that the crystal peak was calculated using the formula for the orthorhombic unit cell as follows:

$$V_0 = abc \quad S_0 = \frac{h^2}{a^2} + \frac{k^2}{b^2} + \frac{l^2}{c^2}$$

$$d_0 = \sqrt{\frac{1}{S_0}} \quad \theta_0 = a \sin\left(\frac{\lambda}{2d_0}\right)$$

where $V_0 = 1.862 \times 10^3$, $d_0 = 5.3$, $2\theta_0 = 16.727°$, and $\lambda = 1.5418$ for Cu Kα. Measurement of WAXD was carried out using a Phillips X-ray diffractometer in the transmission mode, with curved crystal monochromatized radiation of 40 kV and 30 mA.

Crystalline index

A thin, flat bundle of well-parallelized PLA filaments were prepared on the sample holder, to determine the crystalline fraction of as-spun and treated PLA yarns. An equatorial diffraction scan of the sample was obtained by varying 2θ from 10° to 35°, at 1°min^{-1} interval. X-ray intensity profiles of all five samples were presented in Figures 2–6. The crystalline index,[10,11] which is a measure of the crystalline fraction of the material, is defined as the ratio of the crystalline scat-

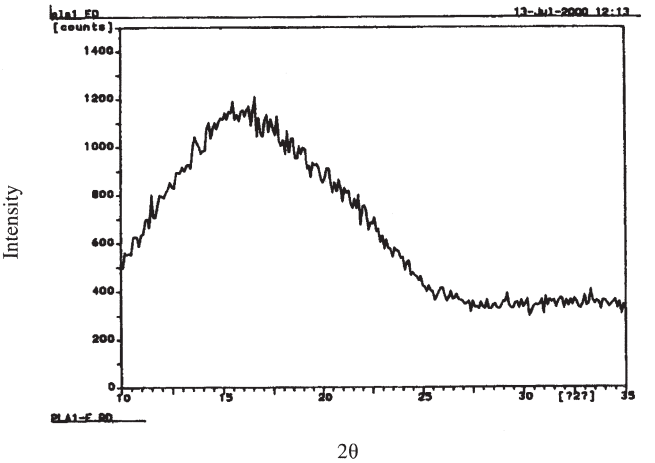

Figure 2 As-spun filaments spun at 500 mm^{-1}.

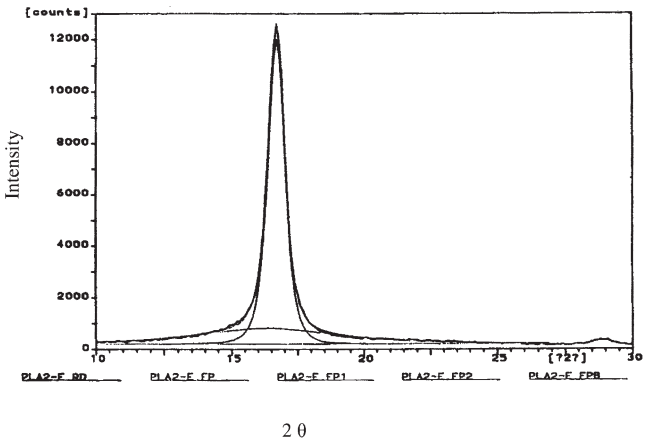

Figure 3 Equatorial scan of drawn and heat-set sample spun at 500 mm^{-1}.

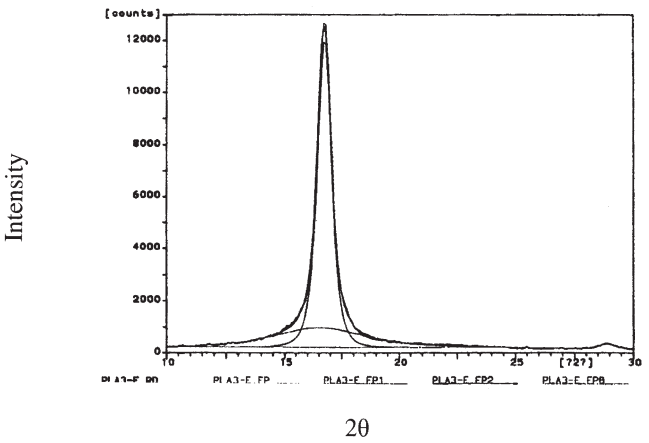

Figure 5 Equatorial scan of drawn and heat-set sample with tension spun at 1850 mm^{-1}.

tering fraction to the total crystalline and amorphous scattering.

Crystal size

The crystallite size was estimated using the width of the crystalline peaks of an equatorial diffraction peak. The crystalline peak at $2\theta = 16.7°$, corresponding to (200) and (100) planes, was analyzed by calculating the width at half maximum intensity. CS was calculated from the Scherrer equation[12] as follows:

$$CS = \frac{K\lambda}{\beta \cos\theta}$$

where K is the shape factor (a constant taken as unity), λ the wavelength of the X-ray (1.5418 Å), and β is the total breadth at half maximum intensity (corrected for instrumental broadening). θ is defined in Bragg's equation.

Crystalline orientation index

Crystalline orientation angle was determined using an azimuthal breadth method.[12] Orientation index was calculated from the breadth at half maximum intensity. The azimuthal scans of the PLA specimens were prepared from a parallelized sample by fixing 2θ at 16.70 (200)(100) arc, which were derived from the diffraction scan. The orientation index (a quantity similar to Hermans' function) was calculated as follows:

$$f_c = (3\ \mathrm{Cos}^2\varphi - 1)/2$$

where f_c is the orientation index and φ is the average of FWHM values of the (200) (110) peak of the azimuthal intensity distribution of the filaments. An av-

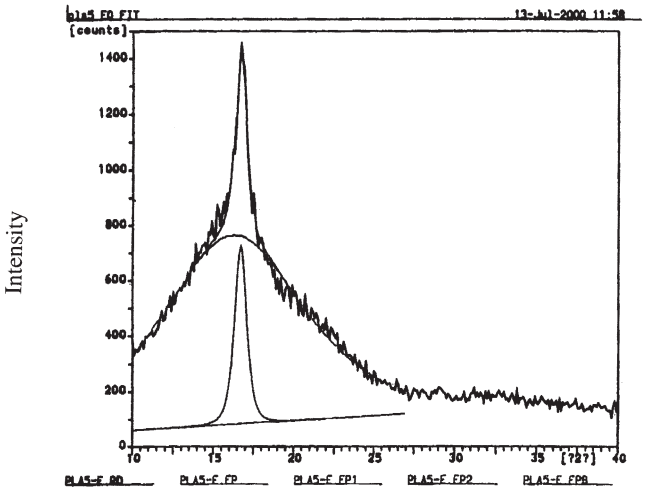

Figure 4 As-spun filament at 1850 mm^{-1} spinning speed.

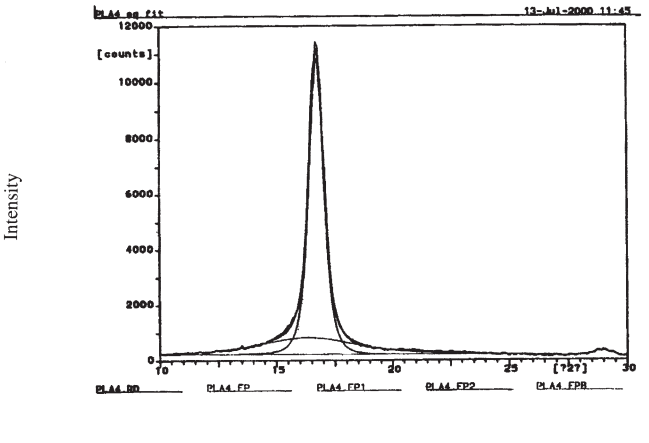

Figure 6 Equatorial scan of drawn, heat-set, and relaxed filaments.

TABLE I
Crystalline Index and Crystal Size of PLA Filaments

Specimen ID	Crystalline fraction (%)	Crystal size of (200) (100) (Å)	Orientation index by X-ray
As-spun at 500 mm^{-1}	Nearly amorphous	—	0.268
Drawn, heat-set, and spun at 500 mm^{-1}	58.40	120.1	0.971
As-spun at 1850 mm^{-1}	6.04	100.4	0.973
Drawn, heat-set, and relaxed spun at 1850 mm^{-1}	59.94	124.3	0.973
Drawn, heat-set, not relaxed spun at 1850 mm^{-1}	59.32	123.9	0.973

erage value of φ for each sample was calculated by scanning from both directions.

Molecular orientation index

Molecular orientation was estimated using acoustic method, by applying sonic velocity and modulus of the PLA filaments. Research studies[13–16] have shown that sound propagation through filaments depends on the molecular orientation of the filaments. High sound velocity through the filament results from the high levels of molecular orientation, with stiff intermolecular bonds that facilitate sound transmission. Sonic modulus is a measure of molecular orientation (composite of amorphous and crystalline phase), because the intermolecular and intramolecular force constants that control filament stiffness are not measurably different for crystalline and amorphous regions in the fiber.[16] Church and Mosley[16] developed a relationship between sonic velocity and modulus as follows:

$$E = 11.3C^2$$

where C is the sonic velocity (K S^{-1}) and E is the sonic modulus (g d^{-1}).

Furthermore, these researchers[13,15,16] also used a molecular orientation index by relating sonic modulus to angle of molecular chain to the fiber axis θ and $\cos^2\theta$, the mean square projection of chains on the fiber axis. The following equation describes the relationship:

$$\alpha = \frac{1}{2}(3\cos^2\theta - 1) = \left[1 - \frac{E_u}{E}\right]$$

where α is the orientation index, E_u the sonic modulus of amorphous material, and E is the sonic modulus of the experimental filaments.

Sonic velocities of the filaments were determined using a Dynamic Modulus Tester PPM-5R. In this study, as-spun filaments made at 500 mm^{-1} were considered as amorphous materials.

RESULTS AND DISCUSSION

The structure development of fibers is usually described by X-ray diffraction methods. Therefore, we performed WAXD to obtain crystallinity, CS, and crystalline orientation index, and the results are presented in Table I. The X-ray diffractogram (Fig. 2) of as-spun filament, spun at 500 mm^{-1} spinning speed, shows a broad halo centered at $2\theta = 16.7°$. This suggests that the yarn spun at 500 mm^{-1} is predominately amorphous. After drawing and heat-setting, the filaments spun at 500 mm^{-1} developed a significant amount of crystallinity (58.40%), and a strong crystalline peak at

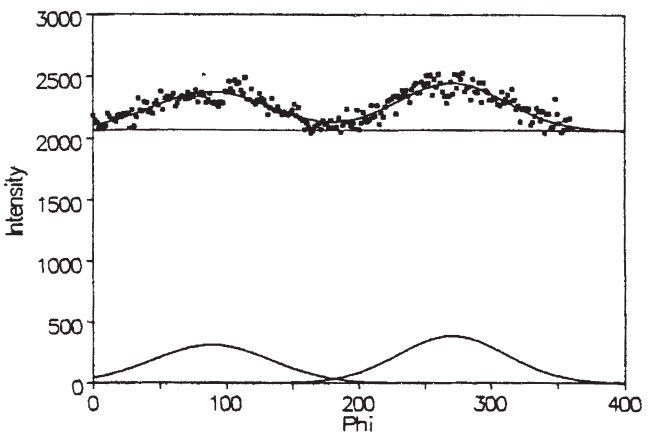

Figure 7 Azimuthal scan of PLA as-spun filaments spun at 500 mm^{-1}.

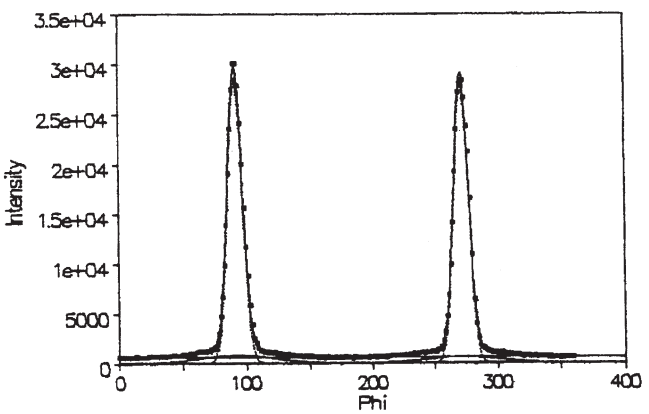

Figure 8 Azimuthal scan of PLA filaments spun at 500 mm^{-1}, drawn, and heat-set.

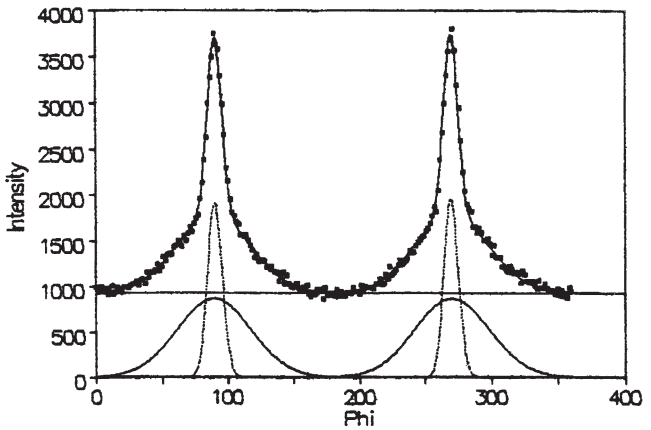

Figure 9 Azimuthal scan of PLA as-spun filament at 1850 mm^{-1}.

$2\theta = 16.7°$ of (200) and (110) reflections was observed in Figure 3. These two reflections were calculated from a diffractogram. The X-ray diffractogram observed for as-spun sample, produced at 1850 mm^{-1} spinning speed, is shown in Figure 4. It is apparent from Figure 4 that crystal reflection can be resolved. Crystallinity of as-spun yarn spun at 1850 mm^{-1} was measured as 6% from the diffraction pattern. The crystallinity value obtained for as-spun PLA filaments, spun at 1850 mm^{-1}, is much lower than drawn and heat-set PLA yarns spun at both spinning speeds (500 and 1850 mm^{-1}).

This crystallinity, developed for as-spun PLA yarns spun at 1850 mm^{-1}, is attributed to the orientation-induced crystallization associated with the entropy of the amorphous, noncrystalline phase. At higher spinning speed, a greater velocity gradient is created in the spin line, which causes stretching and alignment of macromolecules[17] during the development of orientation. This process reduces entropy of the amorphous phase by a certain amount, depending upon the degree of orientation created during spinning. This free energy for crystallization provides a driving force for the kinetics of crystal nucleation and growth of the filaments. Filaments that were spun at both low and high spinning speeds exhibited relatively high level of crystallinity (~60%) after drawing and heat-setting, as expected. This can be attributed to thermal as well as stress-induced crystallization. Since almost same crystallinity was obtained for the PLA yarns after drawing and heat-setting, it was concluded that thermally induced crystallization has the greatest contribution toward the development of filament crystallinity. However, samples drawn with tension rolls without relaxation showed a slightly lower crystallinity than that of the filaments relaxed after drawing. At the heat-setting process, the local melting of small and less stable crystals occurs, and the short length molecules move to form more stable intermolecular bonds that provide better perfection of crystals. This local melting allows recrystallization into folded segments, following the folds that are already present as nuclei for recrystallization. The amount of tension during heat-setting influences the amount of refolding. Very high tension inhibits the folding process and, consequently, disrupts the crystal perfection during the annealing treatment.[18] Furthermore, the relative amounts of mobility of the molecular segments are low under taut condition. CS values are presented in Table I, which show that larger CS's were obtained for samples spun at significantly higher spinning speed and drawn as well as heat-set yarns.

Semicrystalline polymeric fibers can have various levels of molecular orientation, ranging from random distribution to highly align in the fiber axis direction, and the determination of molecular orientation is of great interest from both the technical and theoretical point of view.[19] Molecular orientation includes both crystalline and amorphous orientation, which can be measured using birefringence measurements and acoustic method by sonic velocity and modulus of the PLA filaments. Crystalline orientation can be measured using WAXD or polarized infrared spectroscopy.[20] In this study, crystalline orientation values were obtained from azimuthal scans of the PLA filaments and are illustrated in Figures 7–11. Crystalline orientation values estimated for different PLA filaments, using azimuthal scans, are also included in Table I. The crystalline orientation value of as-spun filaments from 500 mm^{-1} spinning speed represents the amorphous orientation, since the filaments at this manufacturing condition were practically amorphous. For the rest of the sample, the amorphous portion of the material has been separated using computer software, and orientation values were calculated from the crystalline intensity profile only. It should be noted from Figures 8–11 that there are no significant differences in orientation indices in the crystalline fraction of the

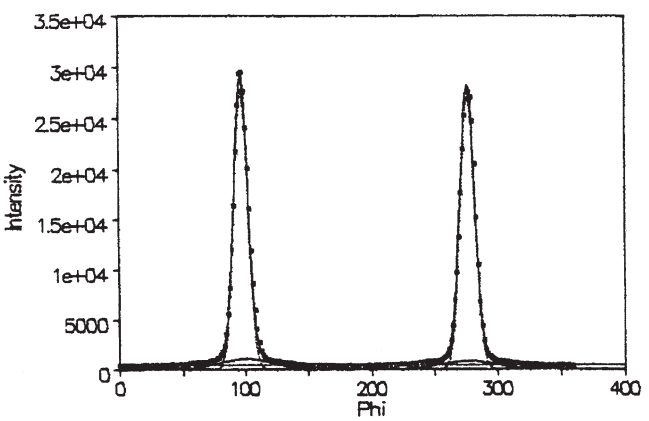

Figure 10 Azimuthal scan of PLA filaments spun at 1850 mm^{-1}, drawn, and heat-set, but not relaxed.

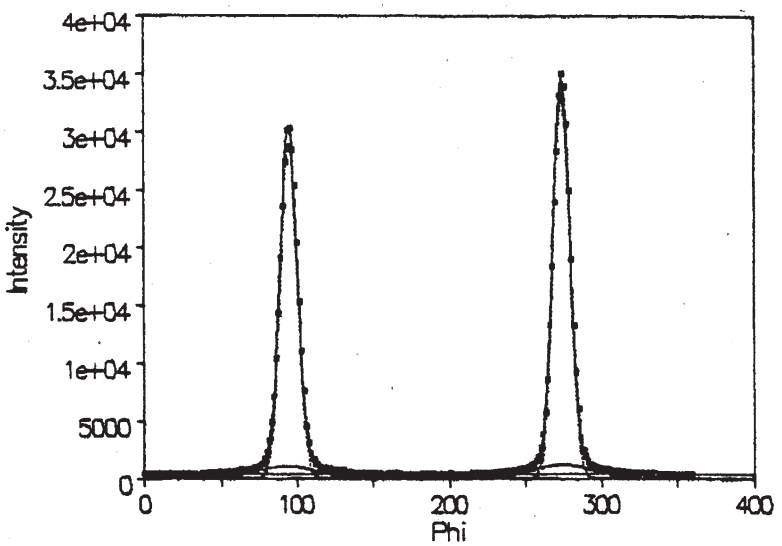

Figure 11 Azimuthal scan of PLA filaments spun at 1850 mm^{-1}(drawn, heat-set, and relaxed).

materials among different samples. When a segment of the chains become parallel to the same segment of the adjacent chains, crystallites are formed, and therefore, orientation of these segments will be high; however, it does not indicate that the overall molecular alignment of the chains (molecular orientation) will necessarily be high.

In our study, sonic velocity was used to measure the molecular orientation. Molecular orientation was low for undrawn samples as expected, and molecular orientation observed for PLA fibers, spun at relatively high speed at 1850 mm^{-1}, is significantly low as seen in Table II. A higher level of molecular orientation was achieved after drawing the filaments. The highest level of orientation was achieved for heat-set filaments under taut condition, which may be attributed to further alignments of the molecular chains, because of the high tension at elevated temperatures during heat-setting.

For many applications, the relatively low glass transition temperature and low modulus of PLA are advantageous. For example, the low T_g permits dyeing at lower temperature than does PET, and the low modulus leads to better handle and drape in textile fabrics. For high performance applications, however, the low T_g and relatively low modulus of PLA are drawbacks. In addition, PLA suffers from an unfavorable rate of hydrolysis above the T_g.

We are addressing these limitations with a view to expanding the use of PLA via preparation of new classes of PLA-based hybrid materials. PLA nanocomposites with different amount of organically modified clay were prepared (2–10%, w/w). Organically modified clay was prepared by standard cation exchange method reported earlier.[21] When clay was modified with an organic compound, it showed an improvement in dispersability. Our preliminary investigation showed a significant increase in mechanical properties, such as initial modulus and elongation at break of the PLA cast undrawn nano composite film, as reported in Table III. Furthermore, there was an increase in T_g when PLA was loaded with 5% clay. Crystallin-

TABLE II
Molecular Orientation by Acoustic Method of the PLA filaments

	Sonic velocity ($K\ S^{-1}$)	Sonic modulus ($g\ d^{-1}$)	Molecular orientation index α
As-spun at 500 mm^{-1}	1.80	36.61	—
Drawn, heat-set, and spun at 500 mm^{-1}	2.56	74.06	0.506
As-spun at 1850 mm^{-1}	1.98	44.30	0.174
Drawn, heat-set, and relaxed and spun at 1850 mm^{-1}	2.61	76.98	0.524
Drawn, heat-set, not relaxed spun at 1850 mm^{-1}	2.68	81.16	0.549

TABLE III
Thermal and Mechanical Properties of Cast Untreated PLA and Composite Film

	T_g (°C)	T_c (°C)	% crystallinity	T_m (°C)	Elongation at break (%)	Initial modulus (MPa)
Neat PLA film	65	93	5	147	600	175
PLLA with 5% modified clay	69	95	10	144	960	250

ity of PLA film increased by adding clay particles, suggesting that dispersed clay particles act as nucleating agents. We are in the process of spinning PLA fibers with different amounts of organically modified clay loading, and the outcome of this work will be reported in the near future.

Summary

Our investigation shows that significant modifications of PLA filament is possible through the modification of spinning parameters, which facilitate the development of desired yarn properties needed for various applications. A briefing on the addition of nanoclay particles has shown that the mechanical properties of PLA composite can be improved. This later portion of our study will be published in future articles.

References

1. Perego, G.; Cella, G. D.; Basttioli, C. J Appl Polym Sci 1996, 195, 1649.
2. Drumright, R. E.; Gruber, P. R.; Henton, D. E. Adv Mater 2000, 12, 1841.
3. De Santis, P.; Kovacs, A. J. Biopolymers 1968, 6, 229.
4. Lunt, J.; Shafer, A. J Ind Text 2000, 29, 191.
5. Hoogsteen, W.; Postema, A. R.; Pennings, A. J.; Ten Brinke, G.; Zugenmier, P. Macromolecules 1990, 23, 634.
6. Eling, B.; Gogolewski, S.; Pennings, A. J. Polymer 1982, 23, 1587.
7. Mezghani, K.; Spruiell, I. E. J Polym Sci Part B: Polym Phys 1998, 36, 1005.
8. Lunt, J. Polym Degrad Stab 1998, 59, 145.
9. Krikorian, V.; Pochan, D. J. Chem Mater 2003, 15, 4317.
10. Cullerton, D. L.; Ellison, M. B. Text Res J 1990, 60, 601.
11. Alexander, L. E. In X-ray Diffraction Methods in Polymer Science; Robert, E., Ed.; Krieger: New York, 1979; p 82.
12. Alexander, L. E. In X-ray Diffraction Methods in Polymer Science; Robert, E., Ed.; Krieger: New York, 1979; p 262.
13. Samuels, R. J. J Polym Sci Part B: Polym Phys 1963, 3, 1741.
14. DeVries, A. J. Pure Appl Chem 1981, 53, 1011.
15. Mosley, W. W. J Appl Polym Sci 1960, 111, 266.
16. Church, W. H.; Mosley, W. W. Text Res J 1959, 29, 525.
17. Ziabicki, A. In Proceedings of Clemson University and Fiber Producer Magazine Conference; Textile Hall, Greenville, SC, July 15–17, 1980; p 1.
18. Statton, W. O. Polym Sci Symp 1971, 32, 219.
19. Salem, D. R.; Vasanthan, N. In Structure Formation in Polymeric Fibers; Salem, D. R., Ed.; Hanser: Munich, 2001.
20. Vasanthan, N.; Salem, D. R. J Polym Sci Part B: Polym Phys 2001, 39, 536.
21. Giannelis, E. P. Adv Mater 1996, 8, 29.